

Comparison of EEG and MEG in source localization of induced human gamma-band oscillations during visual stimulus

Kidist Gebremariam Mideksa, Nienke Hoogenboom, H. Hellriegel, Holger Krause, Alfons Schnitzler, Günther Deuschl, Jan Raethjen, U. Heute, Muthuraman Muthuraman

Angaben zur Veröffentlichung / Publication details:

Mideksa, Kidist Gebremariam, Nienke Hoogenboom, H. Hellriegel, Holger Krause, Alfons Schnitzler, Günther Deuschl, Jan Raethjen, U. Heute, and Muthuraman Muthuraman. 2015. "Comparison of EEG and MEG in source localization of induced human gamma-band oscillations during visual stimulus." In 2015 37th Annual International Conference of the IEEE Engineering in Medicine and Biology Society (EMBC), 25-29 August 2015, Milan, Italy, edited by Sergio Cerutti, Paolo Bonato, Colin J. H. Brennan, Anna Maria Bianchi, and Silvestro Micera, 8119-22. Piscataway, NJ: IEEE. <https://doi.org/10.1109/embc.2015.7320278>.

Nutzungsbedingungen / Terms of use:

licgercopyright

Dieses Dokument wird unter folgenden Bedingungen zur Verfügung gestellt: / This document is made available under these conditions:

Deutsches Urheberrecht

Weitere Informationen finden Sie unter: / For more information see:

<https://www.uni-augsburg.de/de/organisation/bibliothek/publizieren-zitieren-archivieren/publiz/>



Comparison of EEG and MEG in source localization of induced human gamma-band oscillations during visual stimulus*

Mideksa, K.G., Hoogenboom, N., Hellriegel, H., Krause, H., Schnitzler, A., Deuschl, G., Raethjen, J., Heute, U., and Muthuraman, M.

Abstract—High frequency gamma oscillations are indications of information processing in cortical neuronal networks. Recently, non-invasive detection of these oscillations have become one of the main research areas in magnetoencephalography (MEG) and electroencephalography (EEG) studies. The aim of this study, which is a continuation of our previous MEG study, is to compare the capability of the two modalities (EEG and MEG) in localizing the source of the induced gamma activity due to a visual stimulus, using a spatial filtering technique known as dynamic imaging of coherent sources (DICS). To do this, the brain activity was recorded using simultaneous MEG and EEG measurement and the data were analyzed with respect to time, frequency, and location of the strongest response. The spherical head modeling technique, such as, the three-shell concentric spheres and an overlapping sphere (local sphere) have been used as a forward model to calculate the external electromagnetic potentials and fields recorded by the EEG and MEG, respectively. Our results from the time-frequency analysis, at the sensor level, revealed that the parieto-occipital electrodes and sensors from both modalities showed a clear and sustained gamma-band activity throughout the post-stimulus duration and that both modalities showed similar strongest gamma-band peaks. It was difficult to interpret the spatial pattern of the gamma-band oscillatory response on the scalp, at the sensor level, for both modalities. However, the source analysis result revealed that MEG3 sensor type, which measure the derivative along the longitude, showed the source more focally and close to the visual cortex (cuneus) as compared to that of the EEG.

I. INTRODUCTION

Oscillatory brain activity in humans, occurring in the gamma frequency band (30-100 Hz) has been known for many decades [1-4]. However, it became a recent research interest in the combined EEG and MEG studies due to the advancement of non-invasive recording technologies and

analysis tools. The gamma waves reflect the synchronization of cortical cell clusters associated to both motor and cognitive tasks such as learning, memory, and attention. The rhythmic synchronization of neuronal firings in the gamma-band has been claimed to provide the necessary spatial and temporal links that binds the processing together in different brain areas to produce a coherent object representation [5-6]. Several studies have shown that the induced gamma activity, in response to a coherent visual stimulus, is maximal at the occipital and parieto-occipital areas of the brain originating mainly from the visual cortex [7-10].

Although both EEG and MEG record the signals generated by the same sources (electrical currents in the brain), there are some differences between both methods in identifying the underlying source. EEG data is strongly dependent on the head's shape and tissue conductivity causing the electrical potentials to be smeared and attenuated, yielding a poor signal-to-noise ratio, whereas, MEG signals are not affected by tissue conductivity making MEG more suitable in differentiating simultaneously active cortical areas. Moreover, MEG signals recorded with gradiometers are more sensitive to local brain activity than to global activity and they are also less prone to muscle artifacts as compared to that of the EEG signals, which is a crucial point when considering gamma-band activity as there are muscle artifacts occurring at the same frequency band.

Due to the occurrence of muscle artifacts at the same frequency band, the non-invasive detection of these gamma oscillations need a highly optimized paradigm that can induce strong gamma-band activity [11-12]. Thus, in this study we used a task design that has been proven to induce strong visual cortical gamma-band activity [8] and used cuneus, a region of visual cortex that is mainly responsible in the perception of motion, as the region of interest.

This paper investigates the difference between the two modalities (EEG and MEG) in localizing the induced gamma-band activity through the application of a beam-former technique known as DICS, from simultaneously recorded EEG and MEG data. We used the result from our previous MEG study as a validation to compare it to that of the EEG, where we have analyzed the impact of different MEG sensor types (magnetometers (MEG1) and pairs of gradiometers (MEG2 and MEG3)) in localizing the gamma activity and found out that the MEG3 sensor type (102 gradiometers measuring the gradient along the longitude) localizes the source in the region of interest as compared to the other MEG sensor types [13]. Thus, in this study we

*Research supported by SFB 855 Project D2.

Mideksa, K.G. and Heute, U. are with the Institute for Digital Signal Processing and System Theory, Faculty of Engineering, Christian-Albrechts-University of Kiel, 24105 Kiel, Germany. kgm at tf.uni-kiel.de, uh at tf.uni-kiel.de

Hellriegel, H., Deuschl, G., Raethjen, J., and Muthuraman, M. are with the Department of Neurology, Christian-Albrechts-university of Kiel, 24105 Kiel, Germany. h.hellriegel at neurologie.uni-kiel.de, g.deuschl at neurologie.uni-kiel.de, j.raethjen at neurologie.uni-kiel.de, m.muthuraman at neurologie.uni-kiel.de

Hoogenboom, N., Krause, H., and Schnitzler, A. are with the Department of Neurology, Heinrich-Heine University Düsseldorf, 40225 Düsseldorf, Germany. Nienke.Hoogenboom at med.uni-duesseldorf.de, Holger.Krause at med.uni-duesseldorf.de, schnitza at uni-duesseldorf.de

compared MEG3 sensor type to that of the EEG.

II. DATA ACQUISITION

The simultaneous EEG and MEG signals were recorded using the Elekta Neuromag whole-head system. The system consists of 306 MEG sensors and 128 EEG electrodes. The 306 MEG-system contains three sensor types at one location measuring independent information. The first sensor type consists of 102 magnetometers (MEG1) which measure the magnetic flux perpendicular to its surface and the other sensor pairs consist of 204 planar gradiometers which measure the spatial gradient (102 gradiometers measuring the gradient along the latitude (MEG2) and 102 gradiometers measuring the gradient along the longitude (MEG3)). Both the EEG and MEG data were sampled at 1000 Hz. The EEG was re-referenced, offline, to the parieto-occipital electrodes (EEG099 and EEG101).

The protocol is similar to that of our previous study where the experiment was performed by the same five healthy subjects (four females and one male). The experimental procedures in this study were approved by the local Ethics Committee, Medical Faculty, University of Kiel and all subjects gave their informed consent. Their age ranged from 25 to 36 years (31 ± 5.15). Each trial started with the presentation of a fixation point. After a baseline period of 1000 ms, the fixation point was replaced by a foveal circular sine wave grating (diameter: 5; spatial frequency: 2 cycles/deg; contrast: 100%) and made to accelerate contracting towards the fixation point (velocity step to 2.2 deg/s) for 50 to 1500 ms. The subjects were asked to fixate for the entire experiment and press a button with their right index finger within 500 ms of this acceleration. The stimulus was turned off after a response was given and was followed by a resting period of 1000 ms in which subjects were given visual feedback about the correctness of their response and were asked to blink. Each subject completed 80-150 trials. The recording session lasted for about 50 min.

III. METHODS

Three main analysis steps were carried out in order to localize the gamma-band activity in all the subjects: time-course power analysis at the sensor level, head modeling, and source analysis underlying the spectral component obtained from the sensor-level analysis. All the analyses were performed using the FieldTrip open-source Matlab toolbox (<http://fieldtrip.fcdonders.nl/>).

A. Time-Frequency Analysis

To detect the latency and frequency range of the gamma-band activity which are not known a priori, we performed a time-frequency representation (TFR) of the signal. The method is based on multitapering of the signal, which allows a better control of time and frequency smoothing, to reveal the time-varying estimate of the power of the signal at a given frequency [14]. Calculating the TFRs power is done using a sliding time window, where each windowed trial is multiplied with one or more orthogonal tapers (windows) in the

frequency domain and finally averaged. In this study, we also used a 50 ms sliding window and a Hanning taper similar to that of the MEG study. The TFRs power were represented as a percent change with respect to the baseline (1000 ms before stimulus onset, considering 0 ms as the onset onset for the stimulus). We used the data from 1000 ms before stimulus onset until 1500 ms after stimulus onset. Power estimates were averaged across 37 parieto-occipital EEG electrodes (EEG085, EEG087, EEG088, EEG093, EEG094, EEG095, EEG096, EEG097, EEG099, EEG100, EEG101, EEG103, EEG104, EEG105, EEG106, EEG107, EEG108, EEG109, EEG110, EEG111, EEG112, EEG113, EEG114, EEG115, EEG116, EEG117, EEG118, EEG119, EEG120, EEG121, EEG122, EEG123, EEG124, EEG125, EEG126, EEG127, EEG128) and compared it to that of the power estimates averaged across 32 parieto-occipital MEG3 sensor type.

B. Head Modeling

In order to localize neuronal current activity, a valid head model (forward model), which calculates the electromagnetic potentials and fields generated from a current source, is necessary irrespective of the inverse technique used.

The first and the simplest volume conductor models of the human head consisted of a homogeneous sphere. However, since the tissues of the brain have different conductivities, the three-shell concentric spherical head model has been introduced [15]. The outer most sphere represents the scalp, the intermediate sphere represents the skull, and the inner most sphere represents the brain. As we have focused on the spherical head model in our previous MEG study, we have used the three-shell concentric spherical model in this study to calculate the potential field recorded by the EEG electrodes. The potential, \mathbf{V} , at the scalp point, P , for a given dipole (current source) is calculated using the semi-analytic solution of Poisson's equation [16-17]:

$$\mathbf{V} = \frac{1}{4\pi\sigma R^2} \sum_{i=1}^n \frac{X(2i+1)^3}{m_i(i+1)i} r^{i-1} [i d_r P_i(\cos\theta) + d_t P_i^1(\cos\theta)], \quad (1)$$

with m_i given by:

$$m_i = [(i+1)X + i] \left[\frac{iX}{i+1} + 1 \right] + (1-X)[(i+1)X + i] (f_1^{(2i+1)} - f_2^{(2i+1)}) - i(1-X)^2 (f_1/f_2)^{(2i+1)} \quad (2)$$

where $n = 3$, d_r and d_t are the radial and tangential components of the dipole, R is the radius of the scalp, σ is the conductivity of the scalp and the brain (0.33 S/m), X is the conductivity ratio between the skull (0.0041 S/m) and the soft tissue, r is the relative distance of the dipole from the center, θ is the polar angle of the surface point, P_i and P_i^1 are the Legendre and the associated Legendre polynomial, f_1 is the ratio between the brain and the scalp radii, f_2 is the ratio between the skull and the scalp radii.

Estimation of the magnetic field using the local sphere technique for the MEG is explained elsewhere [18]. Since

EEG is affected by the volume conduction effect of the head there is a need to model the different tissues of the brain which leads us in using the three-shell concentric spherical model, unlike MEG where a single sphere suffice.

C. Source Localization

In order to locate the gamma-band activity, we used a beamformer technique known as dynamic imaging of coherent sources (DICS). It is quite often used in localizing the coherent network of sources for a specific frequency band by imaging power and coherence estimates within the brain [19-20]. In this study, we used only the power information to enable us in determining the neuronal current sources underlying the induced gamma activity upon visual stimulation for the identified frequency range. DICS is a data-driven spatial filter which exploits the second order statistical information in the form of the cross spectra of signals. The power and the cross spectra are calculated by applying a Hanning window and Welch's method of periodogram. The spatial filter, \mathbf{A} , as shown in equation (3), is then designed using the cross-spectral density, $\mathbf{\Gamma}$, between all the channels over the frequency range of interest, obtained from the time-frequency analysis, and the leadfields, \mathbf{L} , obtained from the forward modeling, in such a way that the leadfields representing the frequency of interest are strengthened while others are suppressed.

$$\mathbf{A} = [\mathbf{L}^T(\bar{\mathbf{r}})\mathbf{\Gamma}^{-1}\mathbf{L}(\bar{\mathbf{r}})]^{-1}\mathbf{L}^T(\bar{\mathbf{r}})\mathbf{\Gamma}^{-1} \quad (3)$$

The spatial distribution of the power of the neuronal sources is then represented as a contrast with respect to the baseline and overlaid on a structural image of the subject's brain.

IV. RESULTS

A. Time-frequency Analysis

The grand-averaged time-frequency across all trials and across the parieto-occipital electrodes and sensors for both the EEG and MEG showed a sustained gamma-band activity in response to the visual stimulus. Fig. 1A shows the time course of both the EEG and MEG gamma-band activity for one of the representative subjects. It can be seen that the gamma-band activity is maintained throughout the post-stimulus duration. The gamma power, expressed in percent change with respect to the baseline, was different for all the subjects, mainly concentrating between 40-80 Hz. The strongest gamma-band peaks were similar for both modalities. Highest absolute power of the gamma activity is observed in all of the subjects for the case of EEG as compared to the MEG3 sensor type. Taking the average of the time point, where the maximum gamma activity is detected over all the subjects, we have observed that the induced gamma activity is detected a few ms after the stimulus onset using EEG, whereas, it takes a few more ms to be detected using MEG. This absence of the gamma activity in the MEG could be due to the deep and/or radially oriented neuronal sources which cannot be detected by the MEG sensors due to their

weak magnetic field. The topographic maps for the frequency band, obtained from the TFR analysis, showing the strongest gamma-band activity (0 to 1.5 sec), demonstrated a parieto-occipital relative power distribution for both modalities. Fig. 1B shows the result for one of the representative subjects.

B. Source Localization

The maximum gamma-band activity in response to the visual stimulus was localized using the DICS technique for both modalities using each subject's strongest gamma-band frequency peak obtained from the time-frequency analysis. Fig. 2 shows the estimated source power at 72 ± 6 Hz, from the grand average over all the trials for each of the modalities separately, relative to the pre-stimulus baseline activity localized in the early visual areas for one of the representative subjects. Comparing the modalities, MEG3 sensors were able to localize the source close to the visual cortex (cuneus) as compared to EEG for all the subjects. This result was supported by calculating the euclidean distance between the reference MNI coordinate (x,y,z), midline of the cuneus separating the two hemispheres (obtained from the standard template: 2,-86,26 mm) to that of the MNI coordinate of the strongest response (voxel with the highest power occurring either in the right or left hemisphere of the visual cortex) obtained from the source analysis for each subject separately (mean \pm std: MEG3=35.45 \pm 1.9, EEG=47.10 \pm 46.75). Moreover, MEG3 sensors were able to localize the source more focally as compared to EEG. This result was supported, for all the subjects, by estimating the number of voxels activated over the whole brain for each modality (mean: MEG3=5872 \pm 2598.54, EEG=6232 \pm 4134.48). The criterion used to estimate the number of highly activated voxels was by taking those voxels which showed 50% of the highest relative power change with respect to the baseline. The smaller the number of voxels, the more focal we see the source in the expected region of interest, which is the cuneus.

V. CONCLUSIONS

In this study, we have analyzed the difference between the two modalities (EEG and MEG) in localizing the induced gamma activity in response to the visual stimulus using simultaneously recorded EEG and MEG data. We applied the adaptive spatial filtering technique known as DICS to localize the underlying source. From the time-frequency analysis, at the sensor level, we observed that the stimulus related response occurs in the gamma frequency range and that the individual gamma-band frequencies varied between 40-80 Hz. However, all the subjects showed a similar gamma-band peak frequency for both modalities. Moreover, we also observed that the EEG detects the induced gamma activity earlier than MEG, which could be due to the weak magnetic fields generated by the deep and/or radially oriented neuronal sources. Our results at the sensor and source level were compatible in detecting the source around the parieto-occipital areas of the brain. Moreover, the source level analysis revealed additional information in detecting the source more focally and closer to the region of interest, that

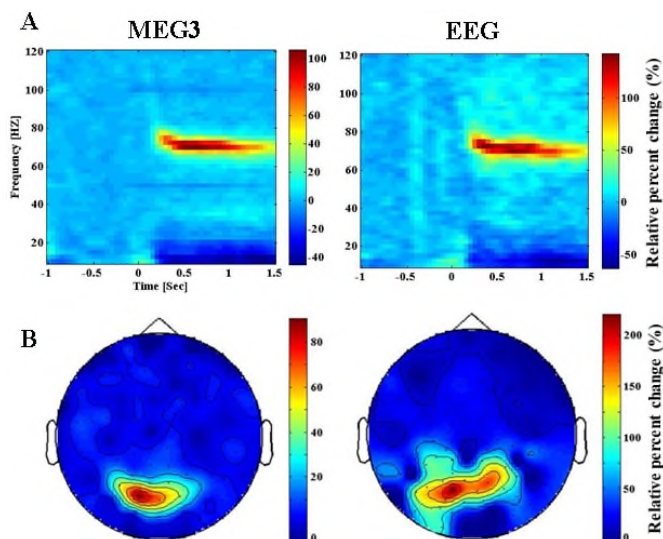


Fig. 1. A. Time-frequency plot of both modalities representing the gamma power across the average of selected parieto-occipital MEG sensors and EEG electrodes, respectively for one of the representative subjects. Baseline: -1 to 0 sec, Stimulus: 0 to 1.5 sec. Left: average of 32 parieto-occipital MEG3 sensors, right: average of 37 parieto-occipital EEG electrodes. B. Sensor level topographic map of gamma-band activity, for the latency of 0 to 1.5 sec, for both MEG3 sensors and EEG electrodes, respectively. The colorbars represent the percent change with respect to the baseline.

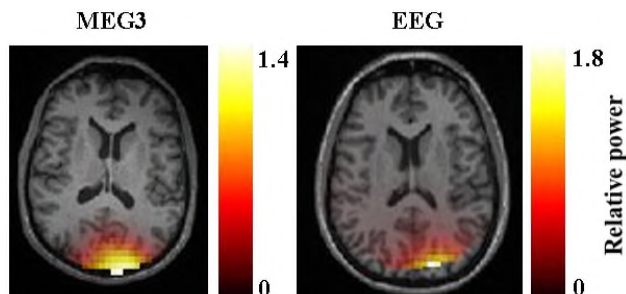


Fig. 2. Estimated sources of visually induced gamma-band activity on a single slice plot of a local sphere head model measured using the MEG3 sensor type in the first column and three-shell concentric spherical head model, in the second column, measured using EEG, for one of the representative subjects. The colorbars indicate the relative power change with respect to the baseline.

is, the cuneus using MEG3 sensor type as compared to the EEG, even though we observed highest absolute power for the case of EEG from the time-frequency analysis.

ACKNOWLEDGMENT

Support from the German Research Council (Deutsche Forschungsgemeinschaft, DFG, SFB 855, Project D2) is gratefully acknowledged.

REFERENCES

[1] H.H. Jasper, H.L. Andrews, *Electroencephalography. III. Normal differentiation of occipital and precentral regions in man*, *Arch. Neurol. Psychiatry*, vol. 39, pp. 96-115, 1938.

[2] C. Krausse, P. Korpilahti, B. Prn, J. Jantti, H.A. Lang, *Automatic auditory word perception as measured by 40 Hz EEG responses*, *Electroencephalogr. Clin. Neurophysiol.*, vol. 107, pp. 84-87, Aug. 1998.

[3] F. Pulvermüller, C. Eulitz, C. Pantev, B. Mohr, B. Feige, W. Lutzenberger, T. Elbert, N. Birbaumer, *High-frequency cortical responses reflect lexical processing: an MEG study*, *Electroencephalogr. Clin. Neurophysiol.*, vol. 98, no. 1, pp. 76-85, Jan. 1996.

[4] A.C. Papanicolaou, D.W. Loring, G. Deutsch, H.M. Eisenberg, *Task-related EEG asymmetries: a comparison of alpha blocking and beta enhancement*, *Int. J. Neurosci.*, vol. 30, no. 1-2, pp. 81-85, Aug. 1986.

[5] W. Singer, A.K. Engel, A.K. Kreiter, M.H. Munk, S. Neuenschwander, P.R. Roelfsema, *Neuronal assemblies: necessity, signature and detectability*, *Trends Cogn. Sci.*, vol. 1, no. 7, pp. 252-261, Oct. 1997.

[6] S.L. Bressler, *The gamma wave: a cortical information carrier?*, *Trends Neurosci.*, vol. 13, no.5, pp. 161-162, May 1990.

[7] P. Adjamian, I.E. Holliday, G.R. Barnes, A. Hillebrand, A. Hadjipapas, K.D. Singh, *Induced visual illusions and gamma oscillations in human primary visual cortex*, *Eur. J. Neurosci.*, vol. 20, no. 2, pp. 587-592, Jul. 2004.

[8] N. Hoogenboom, J.M. Schoffelen, R. Oostenveld, L.M. Parkes, P. Fries, *Localizing human visual gamma-band activity in frequency, time and space*, *Neuroimage*, vol. 29, no. 3, pp. 764-773, Feb. 2006.

[9] A. Hadjipapas, P. Adjamian, J.B. Swettenham, I.E. Holliday, G.R. Barnes, *Stimuli of varying spatial scale induce gamma activity with distinct temporal characteristics in human visual cortex*, *Neuroimage*, vol. 35, no. 2, pp. 518-530, Apr. 2007.

[10] P. Fries, R. Scheeringa, R. Oostenveld, *Finding gamma*, *Neuron*, vol. 58, no. 3, pp. 303-305, May 2008.

[11] S. Yuval-Greenberg, O. Tomer, A.S. Keren, I. Nelken, L.Y. Deouell, *Transient induced gamma-band response in EEG as a manifestation of miniature saccades*, *Neuron*, vol. 58, no. 3, pp. 429-441, May 2008.

[12] E.M. Whitham, et al., *Scalp electrical recording during paralysis: quantitative evidence that EEG frequencies above 20 Hz are contaminated by EMG*, *Clin. Neurophysiol.*, vol. 118, no. 8, pp. 1877-1888, Aug. 2007.

[13] K.G. Mideksa, N. Hoogenboom, H. Hellriegel, H. Krause, A. Schnitzler, G. Deuschl, J. Raethjen, U. Heute, M. Muthuraman, *Impact of head modeling and sensor types in localizing human gamma-band oscillations*, *Conf. Proc. IEEE Eng. Med. Biol. Soc.*, pp. 2217-2220, Aug. 2014.

[14] D.B. Percival, A.T. Walden, *Spectral analysis for physical applications: Multitaper and conventional univariate techniques*, Cambridge, U.K., Cambridge Univ. Press, Chapter 7, pp. 331-374, 1993.

[15] E. Frank, *Electric potential produced by two point current sources in a homogeneous conducting sphere*, *J. Appl. Phys.*, vol. 23, no. 11, pp. 1225-1228, 1952.

[16] J.P. Ary, S.A. Klein, D.H. Fender, *Location of sources of evoked scalp potentials: corrections for skull and scalp thicknesses*, *IEEE Trans. Biomed. Eng.*, vol. 28, no. 6, pp. 447-452, Jun. 1981.

[17] Y. Salu, L.G. Cohen, D. Rose, S. Sato, C. Kufta, M. Hallett, *An improved method for localizing electric brain*, *IEEE Trans. Biomed. Eng.*, vol. 37, no. 7, pp. 699-705, Jul. 1990.

[18] M.X. Huang, J.C. Mosher, R. Leahy, *A sensor-weighted overlapping-sphere head model and exhaustive head model comparison for MEG*, *Phys. Med. Biol.*, vol. 44, no. 2, pp. 423-440, Feb. 1999.

[19] J. Gross, J. Kujala, M. Hämäläinen, L. Timmermann, A. Schnitzler, R. Salmelin, *Dynamic imaging of coherent sources: Studying neural interactions in the human brain*, *Proc. Natl. Acad. Sci. U.S.A.*, vol. 98, no. 2, pp. 694-699, Jan. 2001.

[20] J. Gross, L. Timmermann, J. Kujala, M. Dirks, F. Schmitz, R. Salmelin, A. Schnitzler, *The neural basis of intermittent motor control in humans*, *Proc. Natl. Acad. Sci. U.S.A.*, vol. 99, no. 4, pp. 2299-2302, Feb. 2002.